

Transient Changes in Melt Pool Size in Laser Additive Manufacturing Processes

Pruk Aggarangsi and Jack L. Beuth
Department of Mechanical Engineering
Carnegie Mellon University
Pittsburgh, PA

David D. Gill
Sandia National Laboratories
Albuquerque, MN

Abstract

This research addresses the prediction of transient changes melt pool size in laser-based additive powder fusion processes. Additive processes are designed to deposit features onto an existing part, as a means for more efficient part manufacture or part repair. Melt pool size is a key process characteristic that must be controlled to allow the precise deposition of complex features. An understanding of transient changes in melt pool size is an important part of efforts to control melt pool size in real time, via thermal imaging or other feedback control systems. In this research, a process map approach formerly applied to the analysis of steady-state melt pool size is extended to the study of transient changes in melt pool size due to a step change in laser power or velocity. Changes in melt pool size vs. distance or time are presented in quasi-nondimensional form, allowing results from simulations spanning the range of practical process parameters to be presented in compact form. Process map plots are used to quantify the range of times needed to achieve typically desired melt pool size changes. These times establish lower bounds on response times for any thermal feedback control system.

Introduction

A critical issue for advancing laser-based powder fusion processes for additive manufacturing or component repair applications is the need for a fundamental understanding of transient changes in melt pool size with changes in process variables such as laser power and velocity. This understanding is needed to aid in the real-time feedback control of melt pool size, which has a direct impact on the ability to successfully deposit complex shapes. In particular, knowledge of thermal response times (the time for a step change in power or velocity to produce a desired change in melt pool size) is needed. For example, results presented for thin-walled structures by Aggarangsi et al. (2003) demonstrate that effective control of melt pool size during the approach of a free edge is difficult and requires a full understanding of thermal response times. This is due to the fact that the time needed for the melt pool size to change due to a power reduction is comparable to the time over which the melt pool size increases as the free edge is approached.

The research described in this paper attempts to address this issue. Work described herein builds directly on modeling work by Vasinonta et al. (1999, 2001a, 2001b) developing easy-to-use “process maps” allowing the prediction of steady-state melt pool size in thin-walled and bulky features for any practical combination of LENSTM process variables. The simultaneous control of residual stress and melt pool size has been addressed by Vasinonta et al. (2000). A brief overview of the process map approach to understanding laser-based freeform

fabrication processes is given by Beuth and Klingbeil (2001) and a complete presentation of the process map approach for controlling steady-state melt pool size and residual stress in thin-walled and bulky parts is given by Vasinonta (2002). Most recently, process maps of cooling rates and thermal gradients at the melt pool boundary have been developed with the goal of predicting microstructure (Bontha and Klingbeil, 2003, 2004). Work by Birnbaum et al. (2003, 2004) has used a process map approach to consider the role of process size scale in melt pool size control.

The approaches and results from this earlier work can be used by process engineers to determine, in general, how to modify process variables in order to obtain an ideal melt pool size, control maximum residual stresses and control microstructure. However, in this earlier work, only process control under steady-state conditions is addressed. In this paper, the process map approach is extended to understand the transient response of melt pool size to step changes in laser power or velocity. Results presented herein build on preliminary results presented by Aggarangsi, Beuth and Griffith (2003). Melt pool size thermal response times over the full range of LENSTM process parameters are presented. Melt pool response times establish a lower bound on the response times of thermal feedback control systems.

Numerical Models and the Process Map Approach

Numerical Models:

The models used in this paper are analogous to those developed by Vasinonta (2002) and are nearly identical to those described by Birnbaum et al. (2004) (also in this proceedings volume). As such, only a short description of the models will be given here. A key difference between the models used in this study and those used in the steady-state analyses by Birnbaum et al. (2004) is mesh resolution. Significantly higher mesh resolution in and near the melt pool is needed for the simulations of this study compared to analogous steady-state simulations.

A schematic of the models and geometries analyzed in this study is given in Fig. 1. The first type of model is two-dimensional and represents a thin-walled structure deposited onto a comparatively large base plate that acts as a heat sink. The second geometry is two-dimensional axisymmetric and represents a bulky structure also deposited onto a large base plate. For both geometries, thermal models are of a concentrated moving heat source and do not model the effects of material addition. The absorbed laser power is designated as αQ , where α is the fraction of laser power from the source that is absorbed by the structure.

For the thin-walled geometry, in comparing with experiments and in determining ranges of absorbed laser powers, a value of $\alpha = 0.35$ is used. For the bulky part geometry, a value of $\alpha = 0.70$ is used. Predictions from numerical models assuming these values of α have shown good agreement with melt pool sizes measured via thermal imaging using the LENSTM process (Vasinonta et al., 1999 and Vasinonta, 2002). In both types of models, the successive deposition of layers is not modeled, but the preheating effects of the deposition of prior layers can be approximated via the specification of an elevated uniform temperature in the part and base plate, designated as T_{base} , which exists before the laser begins its travel across the top of the part. In all cases considered in this paper, the part is tall enough such that any increases in height will not change the results. Melt pool size results are also taken when the heat source is sufficiently far from the vertical free edges such that results are independent of the distance from the edges.

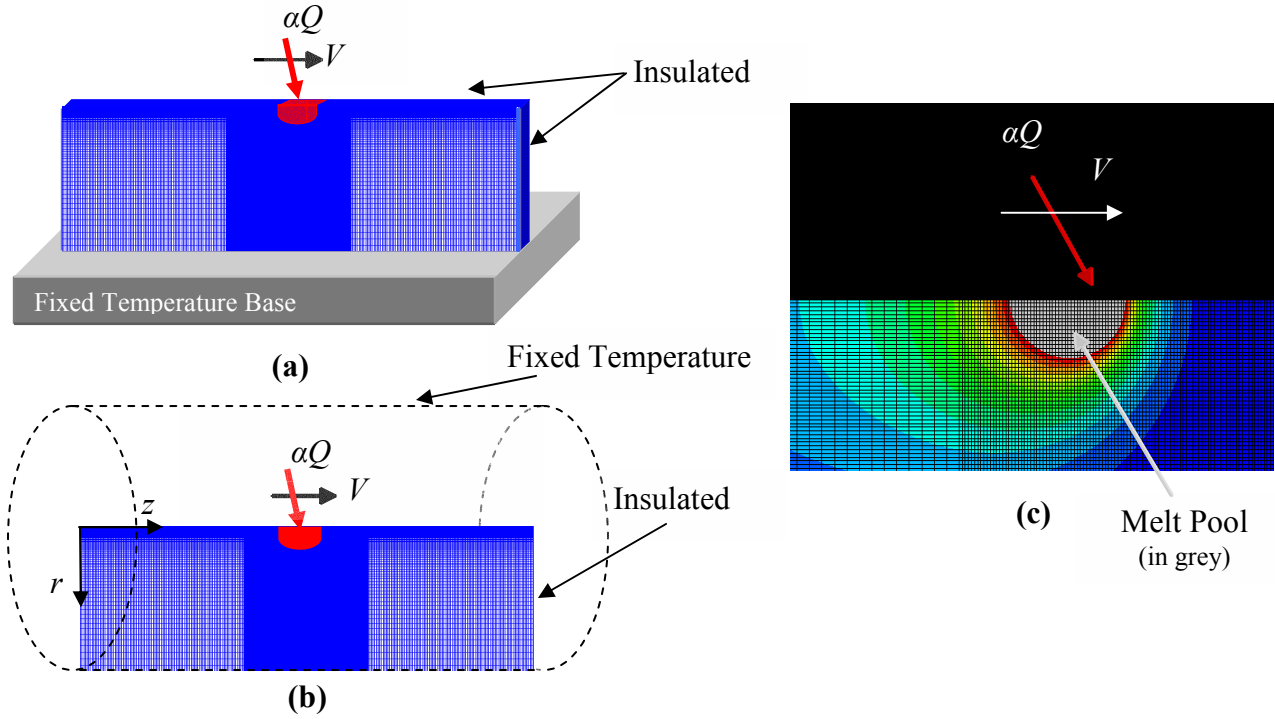


Figure 1. Schematic of (a) Thin-Wall and (b) Axisymmetric Thermal Models and (c) Temperature Contours and Mesh Near the Melt Pool

The mesh used for the bulky part simulations is analogous to that used to model thin walls, except an axisymmetric condition is applied about the axis parallel to the direction of laser displacement (designated as the z axis in Fig. 1b). The axisymmetric model simulates the movement of a heat source through the center of a large solid (modeling double the volume of the actual geometry). Thus, the applied power used in the simulations was twice that suggested by a value of $\alpha = 0.70$. Thermal properties of AISI 304 stainless steel are used as inputs to both types of models (Dobranich and Dykhuizen, 1998). Simulations include temperature-dependent conductivity and specific heat and latent heat effects. Density is treated as a constant. A listing of properties is given by Birnbaum et al. (2004).

Process Map Approach for Steady-State Melt Pool Size: The research on transient changes in melt pool size described herein builds upon previously developed process map concepts. A process map for steady-state melt pool length for a thin-walled structure traversed by a concentrated laser heat source has been developed by Vasinonta et al. (1999, 2001). As suggested by the Rosenthal (1946) solution for a point heat source moving across a (2-D) half-space, a process map for melt pool length is represented through three dimensionless variables: the normalized melt pool length (\bar{l}), the normalized substrate height (\bar{h}) and the normalized melting temperature (\bar{T}_m) which are defined as follows:

$$\bar{l} = \frac{l}{2k/\rho cV}, \quad \bar{h} = \frac{h}{2k/\rho cV} \quad \text{and} \quad \bar{T}_m = \frac{T_m - T_{base}}{\alpha Q/\pi kt}. \quad (1)$$

In eq. (1), ρ , c and k are the density, specific heat and thermal conductivity, respectively. T_{base} is the uniform preheat temperature of the thin wall and base plate upon which the wall is built. αQ

is the laser power imparted to the wall, V is the laser velocity, and t is the wall thickness. If thermal properties are temperature-independent and latent heat effects are not modeled, results from the analysis of a concentrated heat source moving over a thin-walled structure of finite height, h , can be represented as a single surface plotted on three coordinate axes of \bar{l} , \bar{h} and \bar{T}_m . This forms the basis of a process map approach for analyzing the laser deposition of thin-walled structures (under steady-state conditions).

A process map for deposition of thin-walled structures of stainless steel 304 via the LENSTM process can be constructed using results from temperature-dependent thermal simulations including latent heat effects if the following procedures are followed:

1. Properties at 1000 K are used in the normalizations.
2. For cases involving a change in preheat, a linear change in thermal conductivity with preheat temperature (in deg. C) is assumed, given by $k = 24.3 + 0.013(T_{base}-30)$ W/(mK).
3. For predicting steady-state melt pool lengths resulting from a change in process variables, wall thickness is assumed to scale proportionally with melt pool length. The melt pool length/wall thickness scaling is assumed to be unaffected by velocity.

The third assumption is necessary because the wall thickness, t , is included in the normalized variable \bar{T}_m . This requires that some assumption be made regarding the relationship between steady-state melt pool length and wall thickness. For process variables of laser velocity, laser power wall height and preheat temperatures of interest for the LENSTM process, thermal simulation results normalized using the rules above will roughly fall on a single surface plotted on three coordinate axes of \bar{l} , \bar{h} and \bar{T}_m . The variability of results due to temperature-dependent properties can be confined to a range of +/-6.5%.

An analogous approach has been taken to construct process maps for the deposition of bulky parts (Vasinonta, 2002). For such structures, the dimensionless variables are:

$$\bar{d} = \frac{d}{2k/\rho c V}, \quad \bar{h} = \frac{h}{2k/\rho c V} \quad \text{and} \quad \bar{T}_m = \frac{T_m - T_{base}}{\alpha Q / \pi k \left(\rho c V / 4k \right)}, \quad (2)$$

where melt pool depths are considered instead of melt pool lengths and the nondimensionalization for \bar{T}_m no longer includes a thickness, t . It should be noted that the \bar{T}_m definition in eq. (2) differs by a factor of two from the bulky part \bar{T}_m definition used in the studies of microstructure by Bontha and Klingbeil (2003) and Bontha et al. (2004). Normalization procedures needed to collapse thermal simulation results for the LENSTM process onto a single surface in 3-D nondimensional variable space are:

1. Properties of SS304 at 1100 K are used in the normalizations.
2. For cases involving a change in preheat, a linear change in thermal conductivity with preheat temperature (in deg. C) is assumed, given by $k = 25.9 + 0.013(T_{base}-30)$ W/(mK).

If these rules are followed, the variability in melt pool depth results can also be held to within +/-6.5%. The approach of this research is to apply the normalization approaches for steady-state problems outlined above to the transient melt pool size problem.

Targeted Manufacturing Process

Over roughly the past eight years, an extensive research effort at Sandia National Laboratories to develop the LENSTM process (Griffith et al., 1996) has yielded an understanding of process parameters needed to build a number of standard shapes out of stainless steel, titanium and other alloys. Significant progress has also been made in developing real-time feedback control via thermal imaging of the melt pool (Griffith et al., 1999 and Hofmeister et al., 2001). The use of LENSTM for component repair and the integrity of the interfacial bond between the component and newly-deposited material are addressed by Gill and Smugeresky (2004).

Commercially available LENSTM machines currently use a 1kW Nd:YAG laser; however, most of the process development work for the LENSTM process has been performed with systems using a 500 W Nd:YAG laser. This study will focus on the deposition of 304 stainless steel, using process variables corresponding to a 500 W system. The operating power range of a 500 W LENS system is roughly from 150 to 450 W at the laser source. Operating velocities range from 5.93 to 9.31 mm/sec.

Transient Changes in Melt Pool Size for Thin-Walled Structures

In this section, melt pool response to step changes in power or velocity is characterized for the building of thin-walled structures. An initial power level of 300W, yielding $\alpha Q = 105W$ (assuming $\alpha = 0.35$) is used, which is roughly at the midpoint of the operating range for a 500W LENSTM system. Results are presented for the full range of preheat temperatures and velocities for this process. A process map approach is used to condense results from many simulations to characterize melt pool response in a general way.

In considering transient changes in melt pool size, an accounting of changing wall thickness is not needed. The primary effect of an increase in wall thickness is to increase the volume of material available to conduct heat away from the melt pool. While wall thickness will begin to change locally with transient changes in melt pool size, the thickness of the bulk of the wall, which determines the ability to conduct heat away from the melt pool, will not change. In all cases considered in this section, a wall thickness of 1.3 mm is used.

Response to Abrupt Changes in Laser Power: Figure 2 summarizes results characterizing melt pool size changes due to a step change in laser power. The plot is of normalized melt pool length, \bar{l} , vs. normalized distance, \bar{x} , of laser travel after the step change in power is made. An initial power of $\alpha Q = 105W$, a wall thickness of 1.3 mm, a preheat temperature of $T_{base} = 303K$ and thermal properties of SS304 at 1000K yields an initial value of \bar{T}_m equal to 1.29, with an initial value of $\bar{l} = 1.01$. Results presented in Figure 2 include four cases of step changes in laser power by considering increases in laser power of +/-10% and +/-50%. The resulting final values of \bar{T}_m are 0.86, 1.18, 1.44 and 2.59.

Each case of laser power change includes both $T_{base} = 303$ and $T_{base} = 673$ K results and results for velocities equal to 5.93, 7.62, 9.31 mm/sec, covering the full range of process preheat temperatures and velocities. Laser powers applied to a preheated model must be modified slightly in order to maintain the same initial and final values of \bar{T}_m . Values of \bar{x} can easily be converted into actual laser travel distances, x . Elapsed times after a power change is made can

be obtained by dividing x by the laser velocity, V . For reference, elapsed times of 0.1, 0.5 and 1.0 seconds for no preheating and a laser velocity of 7.62 mm/sec have been indicated by vertical dashed lines in the plot of Fig. 2.

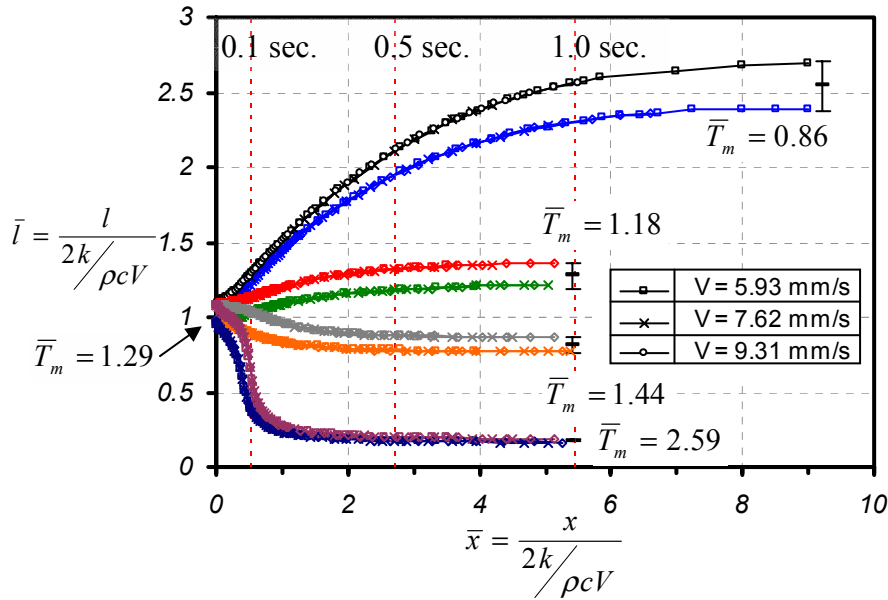


Figure 2. Normalized Melt Pool Length (\bar{l}) vs. Normalized Distance from the Location of a Step Change in Laser Power (\bar{x}) for a Thin-Walled Structure

In Fig. 2, initial and final \bar{l} values for all cases (at steady-state) agree with \bar{l} values from the steady state process map developed by Vasinonta et al, (2001b). The percentage variability in \bar{l} values for transient \bar{l} vs. \bar{x} results does not always match the variability seen in the steady-state results; however, the process map approach originally developed for steady-state problems successfully collapses transient melt pool size results onto essentially four curves. Most of the variability in normalized results comes from differences in preheat temperatures. For each power change case, normalized melt pool length results for the three different velocities are almost indistinguishable. Because \bar{l} vs. \bar{x} results are independent of velocity, differences in non-normalized l vs. x or l vs. time results are almost entirely due to differences in velocity. A larger V reduces the distance that must be traveled to reach a new steady-state melt pool size and it reduces time needed to travel that distance.

Some of the curves in Fig. 2 exhibit an “s” shape (particularly the 50% power reduction case), which indicates reduced changes in melt pool length at times soon after the power change is made. This behavior is caused by changes in melt pool shape. The rate of change in melt pool volume is, as expected, initially large, and then diminishes as laser travel distance or time increases. However, the ratio of melt pool length to melt pool depth does not remain constant, and changes in melt pool length are initially less than changes in melt pool depth. The curves plotted in Fig. 2 clearly demonstrate that for the same percent power change, power increases result in larger \bar{x} values to reach steady state than power decreases.

Table 1 gives numerical values for the normalized distances and elapsed times needed to reach steady state. In this case, steady state is defined as when the melt pool has experienced

90% of the change in melt pool length between the initial and final states. The range of times required to reach steady state is 0.1 - 1.9 seconds.

Table 1. Normalized Distances and Actual Times Required to Achieve 90% of the Melt Pool Length Change due to Step Changes in Power Applied to Thin-Walled Structures

Power Change Cases		Normalized Distance to Achieve 90% of Melt Pool Length Difference	Actual Time to Achieve 90% of Melt Pool Length Difference V = 5.93 mm/s	Actual Time to Achieve 90% of Melt Pool Length Difference V = 9.31 mm/s
50 % Increase	Non-preheat	4.7	1.4	0.6
	Preheat	5.3	1.9	0.8
10 % Increase	Non-preheat	2.4	0.7	0.3
	Preheat	3.0	1.1	0.4
10 % Decrease	Non-preheat	2.3	0.7	0.3
	Preheat	2.3	0.8	0.3
50% Decrease	Non-preheat	0.9	0.3	0.1
	Preheat	1.0	0.4	0.1

Response to Abrupt Changes in Laser Velocity: Figure 3 provides a plot analogous to that of Fig. 2, except that step changes in velocity are considered. In each case, an initial value of $\alpha Q = 105\text{W}$, an initial velocity of 7.62 mm/s and a wall thickness of 1.3 mm are used. Cases with preheat temperatures of $T_{\text{base}} = 303\text{K}$ and $T_{\text{base}} = 673\text{ K}$ are considered (with a slight modification in αQ for the case of $T_{\text{base}} = 673\text{ K}$ to maintain an initial value of $\bar{T}_m = 1.29$). Melt pool size is changed by a step change in laser velocity to either 5.93 or 9.31 mm/s .

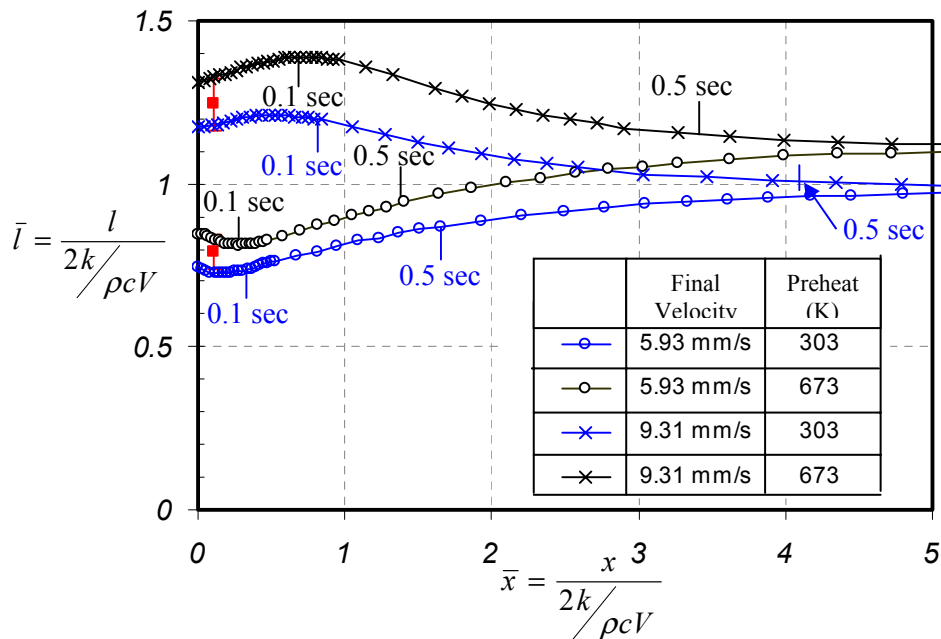


Figure 3. Normalized Melt Pool Length (\bar{l}) vs. Normalized Distance from the Location of a Step Change in Laser Velocity (\bar{x}) for a Thin-Walled Structure

In Fig. 3, results for \bar{x} are normalized by the new velocity. This results in an immediate jump in \bar{l} at the time that the velocity is changed (at $\bar{x} = 0$). At this time, the actual melt pool length has not changed, but the normalized melt pool length is changed by the change in

normalized velocity. In contrast with laser power change cases, velocity changes do not cause any change in \bar{T}_m . As a result, the final value of \bar{l} at steady state will equal the initial value of \bar{l} , and the \bar{l} vs. \bar{x} curve will approach this value as \bar{x} is increased. In the figure, curves at the top of the plot are for cases of switching velocity to 9.31 mm/s. Curves at the bottom of the plot are for switching velocity to 5.93 mm/s. As in the power change simulations, steady-state results match those from (Vasinonta et al. 2001b). The percent variability in results under transient conditions is not always equal to that for steady-state conditions, but the normalization of results is allowing multiple simulations to be represented in a unified way. For reference, short vertical lines indicate elapsed times of 0.1 and 0.5 seconds for each preheat and velocity case. Table 2 quantifies thermal response times from Fig. 3, defining the time to reach steady state as that needed to achieve 90% of the melt pool size change.

A comparison of the results in Figs. 2 and 3, shows that the changes in melt pool length due to the two velocity changes are comparable to those from the +/-10 percent changes in laser power. The normalized distances to reach steady-state for the power change and velocity change cases also appear to be comparable in the figures; however, the numbers given in Tables 1 and 2 suggest larger values of \bar{x} to reach steady state for the velocity change cases. Compared to the laser power change simulations, the velocity change simulations show much greater changes in melt pool shape, which is the reason for the initial increases in melt pool length for a velocity increase and the initial decreases in melt pool length for a velocity decrease. The times to reach steady state for the velocity change cases fall within the range of times to reach steady-state for the power change cases. As a result, the range of response times of 0.1 to 1.9 seconds still holds for the deposition of thin-walled structures via the LENSTM or other similarly sized processes.

Table 2. Normalized Distances and Actual Times Required to Achieve 90% of the Melt Pool Length Change due to Step Changes in Velocity Applied to Thin-Walled Structures

Velocity Change Cases From 7.62 mm/s to		Normalized Distance to Achieve 90% of Melt Pool Length Difference	Actual Time to Achieve 90% of Melt Pool Length Difference V = 5.93 mm/s	Actual Time to Achieve 90% of Melt Pool Length Difference V = 9.31 mm/s
5.93 mm/s	Non-preheat	3.5	1.1	-
	Preheat	3.8	1.4	-
9.31 mm/s	Non-preheat	5.1	-	0.6
	Preheat	4.2	-	0.6

Transient Changes in Melt Pool Size for Bulky Structures

In this section, changes in melt pool size in response to step changes in laser power are considered for bulky structures using methods analogous to those used for thin walls. Step changes in laser velocity have not yet been considered, nor has the effect of different steady velocities on step changes in power. In considering the deposition of bulky structures, a value of $\alpha = 0.70$ is used to determine appropriate initial power and \bar{T}_m values. In the analysis of bulky structures, melt pool depth is used as the characteristic variable defining melt pool size, as suggested in the steady state process map work of Vasinonta (2002). Melt pool depth values are smaller compared to melt pool length values obtained for thin-walled structures (even with α doubled), primarily due to more volume of material available to conduct away heat.

Figure 4 provides a plot of normalized melt pool depth, \bar{d} , vs. normalized distance traveled after a step change in power, \bar{x} , analogous to the plot of \bar{l} vs. \bar{x} given in Fig. 2. Because an appropriate value of α for bulky structures is 0.70, the initial power level corresponding to 300 W at the laser source is $\alpha Q = 210$ W. This power, with a laser velocity, $V = 7.62$ mm/s, a uniform preheat temperature, $T_{base} = 303$ K, and thermal properties of SS304 at 1100 K yields an initial value of $\bar{T}_m = 1.54$. Results presented in Fig. 4 include 4 cases of +/- 10% and +/- 50% laser power changes with final values of $\bar{T}_m = 1.03, 1.40, 1.71$ and 3.08 . Although different velocities have not been considered, preheat temperatures of 303 K and 673 K have been simulated.

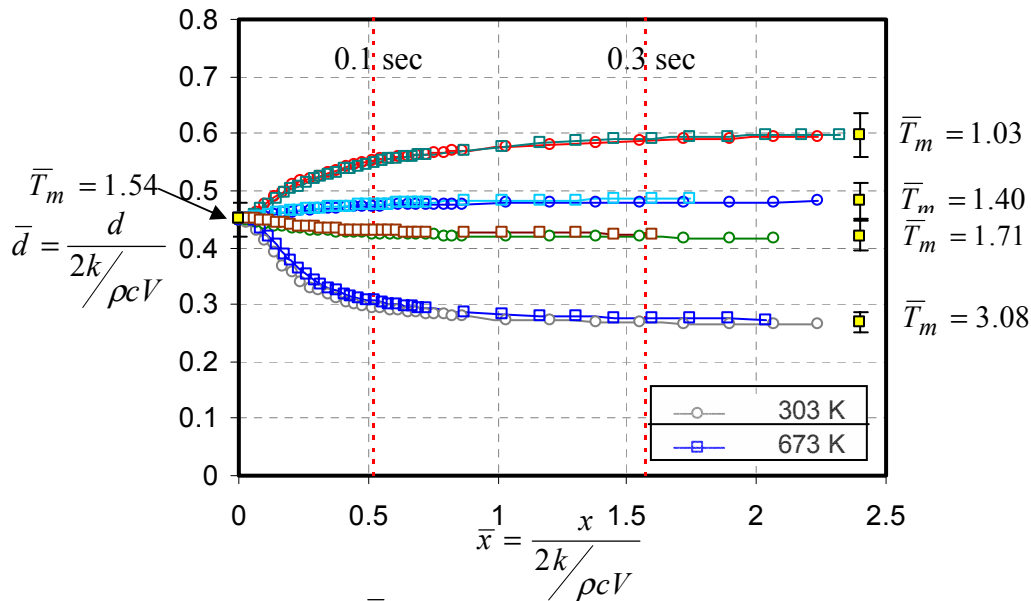


Figure 4. Normalized Melt Pool Depth (\bar{d}) vs. Normalized Distance from the Location of a Step Change in Laser Power (\bar{x}) for a Bulky Structure

Under steady-state conditions, the normalized melt pool depth results of Fig. 4 are well within the variability limit of +/- 6.5% cited by Vasinonta (2002) and indicated on the far right of the plot for each of the final states. Variability in transient preheat and non-preheat results is roughly the same as that for the steady-state results. As for thin-walled structures, the process map approach of collapsing results from multiple simulations, developed for steady state problems, appears to be working under transient conditions also. Overall, there is less of an effect of changes in melt pool shape on melt pool depth results than was seen for melt pool lengths in the thin-walled cases. Also, the percent changes in melt pool size are significantly smaller than were seen for the thin-walled cases.

Table 3 quantifies the normalized distances and actual times to reach steady state. Values in Table 3 are significantly smaller than those in Tables 1 and 2 for thin-walled structures, yet a lower bound on response times of 0.1 seconds still applies. As for the thin-walled cases, normalized distances to reach steady state are smaller for power reduction cases than for power increase cases, though the differences are not as great as was seen in the thin wall cases.

Applications of the Results

Example Calculations Using the Results: Normalized results presented in this paper have been used to determine the time required to reach a new steady state melt pool size for a specified change in laser power or velocity. Results can also be used to determine power changes needed to obtain desired melt pool size changes within a specified period of time. For instance, for cases of an increase in laser power, melt pool transient response time can be reduced by temporarily applying a higher laser power than would be suggested by steady-state process map results.

Table 3. . Normalized Distances and Actual Times Required to Achieve 90% of the Melt Pool Depth Change due to Step Changes in Velocity Applied to Bulky Structures

Power Change Cases		Normalized Distance to Achieve 90% of Melt Pool Depth Difference (V = 7.62 mm/s)	Actual Time to Achieve 90% of Melt Pool Depth Difference (V = 7.62 mm/s)
50 % Increase	Non-preheat	1.2	0.2
	Preheat	1.2	0.3
10 % Increase	Non-preheat	1.0	0.2
	Preheat	0.9	0.2
10 % Decrease	Non-preheat	0.8	0.2
	Preheat	0.8	0.2
50% Decrease	Non-preheat	0.7	0.1
	Preheat	0.8	0.2

As an example, using the results plotted in Figure 3 and tabulated in Table 1, it can be seen that a 10% increase in power (from a value of $\alpha Q = 105$ W and $\bar{T}_m = 1.29$ to $\alpha Q = 116$ W and $\bar{T}_m = 1.18$) results in a change in normalized melt pool length from $\bar{l} = 1.01$ to $\bar{l} = 1.25$. For a laser velocity of 7.62 mm/s, this change in melt pool length occurs over approximately 0.5 seconds. This response time can be reduced by temporarily applying a larger laser power. As indicated in Fig. 3, if instead a 50% increase in laser power is made (to $\alpha Q = 158$ W and $\bar{T}_m = 0.86$), the time needed to reach $\bar{l} = 1.25$ is reduced to approximately 0.1 second. As a result, a more effective control approach for this case would be to apply (at the laser source) $Q = 450$ W of power for roughly 0.1 second and then adjust back to a source power of $Q = 330$ W.

Comparison with Thermal Imaging Experiments: Figure 5 provides a plot of measured melt pool area vs. time for deposition of a stainless steel thin-walled structure via the LENSTM process, during an abrupt change in laser power. Measurements were made using a thermal imaging system used for process analysis and for process feedback control experiments. The laser velocity was 8.39 mm/s. The dotted line in the plot shows the change in power at the laser source, where a value of 40 amps corresponds to 343 W ($\alpha Q = 120$ W for $\alpha = 0.35$) and a value of 44 amps corresponds to 402 W ($\alpha Q = 141$ W for $\alpha = 0.35$). This 17% increase in laser power induces an increase in melt pool area (indicated by the solid line) to a new steady-state value in roughly 0.1 – 0.2 seconds.

Although the starting power and percent power change in this example do not match those analyzed in this paper, the time to reach steady state is comparable to the times to reach steady state indicated in Fig. 3 and Table 1. The results of Fig. 5 also highlight the difficulty in

measuring actual response times experimentally. Even under ideal experimental conditions, fluctuations in the size of the melt pool make identification of response times difficult. Even if experiments are used to map out melt pool response times, plots like those of Figs. 3, 4 and 5 can be useful tools in predicting and interpreting experimental trends.

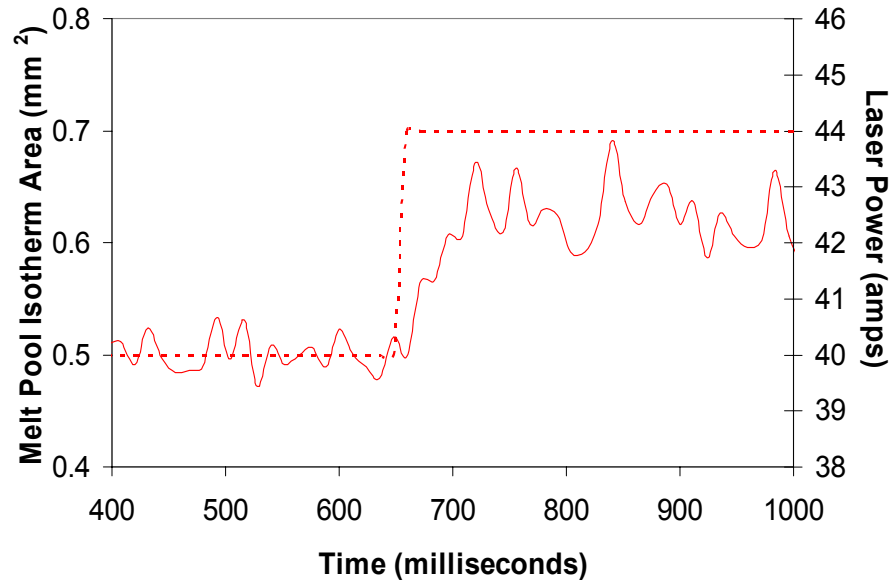


Figure 5. Typical Plot of Melt Pool Area (Solid Line) Measured via Thermal Imaging vs. Time for an Abrupt Change in Laser Power (Dashed Line) (Courtesy of William Hofmeister and Sandia National Laboratories)

Conclusions

In this study a process map approach originally developed for the analysis of steady-state problems is used to characterize melt pool size changes due to abrupt changes in laser power and laser velocity. A single initial power value near the middle of the LENSTM operating range has been considered; however, the full range of possible power and velocity changes for the LENSTM process has been modeled. For thin-walled structures, transient response times from 0.1 to 1.9 seconds have been found. For the deposition of bulky structures, response times range from 0.1 to 0.3 seconds. These thermal response times define a lower bound for the response times of any thermal feedback control system.

Acknowledgements

This modeling research was supported by the National Science Foundation Division of Design, Manufacture and Industrial Innovation, through the Materials Processing and Manufacturing Program, award number DMI-0200270. The authors would like to thank William Hofmeister of Vanderbilt University and Sandia National Laboratories for providing thermal imaging results.

References

1. Aggarangsi, P., Beuth, J.L., and Griffith, M.L., 2003, "Melt Pool Size and Stress Control for Laser-Based Deposition Near a Free Edge," *Solid Freeform Fabrication Proceedings*, Austin, August 2003, pp. 196-207.
2. Beuth, J.L. and Klingbeil, N.W., 2001, "The Role of Process Variables in Laser-Based Direct Metal Solid Freeform Fabrication," *JOM*, September 2001, pp. 36-39.

3. Birnbaum, A., Aggarangsi, P. and Beuth, J.L., 2003, "Process Scaling and Transient Melt Pool Size Control in Laser-Based Additive Manufacturing Processes," *Solid Freeform Fabrication Proceedings*, Austin, August 2003 pp. 328-339.
4. Birnbaum, A., Beuth, J.L., and Sears, J.W., 2004, "Scaling Effects in Laser-Based Additive Manufacturing Processes," *Solid Freeform Fabrication Proceedings*, Austin, August 2004 (in the current proceedings).
5. Bontha, S. and Klingbeil, N.W., 2003, "Thermal Process Maps for Controlling Microstructure in Laser-Based Solid Freeform Fabrication," *Solid Freeform Fabrication Proceedings*, Austin, August 2003, pp. 219-226.
6. Bontha, S., Brown, C., Gaddam, D., Klingbeil, N.W., Kobryn, P.A., Fraser, H.L., and Sears, J.W., 2004, "Effects of Process Variables and Size Scale on Solidification Microstructure in Laser-Based Solid Freeform Fabrication of Ti-6Al-4V," *Solid Freeform Fabrication Proceedings*, Austin, August 2004 (in the current proceedings).
7. Dobranich, D. and Dykhuizen, R. C., 1998, "Scoping Thermal Calculation of the LENS™ Process," Sandia National Laboratories Internal Report, 1998.
8. Gill, D.D. and Smugeresky, J.E., 2004, "Interfacial Strength of LENS Deposited Repair Geometries," *Solid Freeform Fabrication Proceedings*, Austin, August 2004 (in the current proceedings).
9. Griffith, M.L., Keicher, D.M., Atwood, C.L., Romero, J.A., Smugeresky, J.E., Harwell, L.D. and Greene, D.L., 1996, "Freeform Fabrication of Metallic Components Using Laser Engineered Net Shaping (LENS)," *Solid Freeform Fabrication Proceedings*, Austin, August 1996, pp. 125-132.
10. Griffith, M. L., Schlienger, M. E., Harwell, L. D., Oliver, M. S., Baldwin, M. D., Ensz, M. T., Smugeresky, J. E., Essien, M., Brooks, J., Robino, C. V., Hofmeister, W. H., Wert, M. J. and Nelson, D. V., 1999, "Understanding Thermal Behavior in the LENS™ Process," *Journal of Materials Design*, Vol.20, No. 2/3 pp. 107-114.
11. Hofmeister, W.H., Griffith, M.L., Ensz, M.T. and Smugeresky, J.E., 2001, "Solidification in Direct Metal Deposition by LENS Processing," *JOM*, Vol. 53, No. 9, 2001, pp. 30-34.
12. Rosenthal, D., 1946, "The Theory of Moving Sources of Heat and Its Application to Metal Treatments," *Transactions of ASME*, Vol. 68, 1946, pp. 849-866.
13. Vasinonta, A., Beuth, J. L. and Griffith, M. L., 1999, "Process Maps for Laser Deposition of Thin-Walled Structures," *Solid Freeform Fabrication Proceedings*, Austin, August 1999, pp. 383-391.
14. Vasinonta, A., Beuth, J.L. and Griffith, M.L., 2000, "Process Maps for Controlling Residual Stress and Melt Pool Size in Laser-Based SFF Processes," *Solid Freeform Fabrication Proceedings*, Austin, August 2000, pp. 200-208.
15. Vasinonta, A., Beuth, J. L. and Griffith, M. L., 2001a, "A Process Map for Consistent Build Conditions in the Solid Freeform Fabrication of Thin-Walled Structures," *Journal of Manufacturing Science and Engineering*. Vol. 123, pp. 615-622.
16. Vasinonta, A., Beuth, J.L., and Ong, R., 2001b, "Melt Pool Size Control in Thin-Walled and Bulky Parts via Process Maps," *Solid Freeform Fabrication Proceedings*, Austin, August 2001, pp. 432-440.
17. Vasinonta, A., 2002, "Process Maps for Melt Pool Size and Residual Stress in Laser-based Solid Freeform Fabrication," Ph.D. Thesis, Carnegie Mellon University, May 2002.